Solar-Terrestrial Physics. 2026, vol. 12, iss. 2, pp. 49–56. DOI: 10.12737/stp-122202606. © 2026 V.L. Yanchukovsky, V.S. Kuzmenko, R.Z. Khisamov. Published by INFRA-M Academic Publishing House

DOI: 10.12737/stp-122202606
EDN: FJFJYC

Received September 08, 2025
Accepted November 25, 2025

THE MID-LATITUDE ATMOSPHERE OF THE EUROPEAN-ASIAN REGION DURING FORBUSH DECREASES IN COSMIC RAYS

V.L. Yanchukovsky
Trofimuk Institute of Petroleum Geology and Geophysics SB RAS, Novosibirsk, Russia, YanchukovskiyVL@ipgg.sbras.ru

V.S. Kuzmenko
Trofimuk Institute of Petroleum Geology and Geophysics SB RAS, Novosibirsk, Russia, KuzmenkoVS@ipgg.sbras.ru

R.Z. Khisamov
Trofimuk Institute of Petroleum Geology and Geophysics SB RAS, Novosibirsk, Russia, KhisamovRZ@ipgg.sbras.ru

Abstract. The response of the mid-latitude atmosphere to Forbush decreases in galactic cosmic rays is analyzed. We use the results of long-term observations of cosmic ray variations and changes in atmospheric parameters at seven mid-latitude cosmic ray stations for the period from 1966 to 2024. During Forbush decreases (at the decline and minimum of intensity), an increase in atmospheric pressure is observed at all mid-latitude cosmic ray stations. When the cosmic ray intensity is restored after a Forbush decrease, the pressure decreases. The duration of this atmospheric response coincides with the duration of the Forbush decrease. The effect is more pronounced in the cold season, as well as for cosmic ray stations with small geomagnetic cutoff rigidity values. Variations in mean mass and surface temperatures during a Forbush decrease are observed at all cosmic ray stations and differ significantly for the cold and warm seasons. The obtained results suggest that changes in cloudiness and atmospheric transparency caused by changes in the ionization rate during Forbush decreases are a possible cause of the observed effects.

Keywords: cosmic rays, atmosphere, Forbush decreases, pressure, temperature.

INTRODUCTION

In recent years, a significant number of works have been published on the effect of solar activity and related disturbances of the interplanetary medium on the lower atmosphere. There are also works, such as [Erlykin et al., 2009, 2011], where this effect is questioned. One of the reasons for this ambiguity in conclusions may be the involvement of not one, but many factors simultaneously affecting the atmosphere and reflecting changes in solar activity. Increasingly greater attention is currently being paid to cosmic rays (CRs), which are considered as the main source of atmospheric ionization at altitudes from 3 to 50 km. Recent studies suggest that there is a noticeable response to CR variations in atmospheric parameters, such as cloudiness [Pudovkin, Veretenenko, 1995], precipitation [Kniveton, 2004], tropospheric temperature [Pudovkin et al., 1996, 1997], transparency [Roldugin, Tinsley, 2004; Kudryavtsev, Jungner, 2011], etc. It was shown [Dickinson, 1975; Kondratyev, Nikolsky, 1983; Pudovkin, Raspopov, 1992, 1993] that the observed changes in atmospheric cloudiness and transparency occur due to changes in CR intensity, which determine the ionization rate in the lower atmosphere. The above works allow us to assume that ionization of the atmosphere by CRs is one of the links in solar-atmospheric connections, and therefore the research into the CR effects in the behavior of the lower atmosphere parameters is particularly relevant. Continuous time changes in CR flux caused by its modulation in the heliosphere will regulate the contribution of cosmic rays to ionization of the lower atmosphere under changes in solar activity. For high latitudes, the relationship between the evolution and dynamics of pressure systems and CR variations was analyzed in [Veretenenko, Thejll, 2008; Veretenenko, Ogurtsov, 2012], using data from stations in the North Atlantic region: Tasiilag (65.5° N, 38° W) on the southeastern coast of Greenland, Thorshavn (62° N, 6.5° W) on the Faroe Islands, and Jagersborg (56° N, 12° E) in Denmark. These works focused on the spatial distribution of the atmospheric response to Forbush decreases (FDs) in CRs and to solar proton events. At high latitudes, due to low geomagnetic cutoff thresholds, high amplitudes of CR variations are observed. This leads to the fact that CR effects in the evolution of pressure systems at high latitudes are manifested on a larger scale [Veretenenko, Thejll, 2008; Veretenenko, Ogurtsov, 2012]. Accordingly, it should be expected that the atmospheric response (changes in pressure, temperature, cloudiness, etc.) to changes in solar activity may vary from region to region. Yanchukovsky [2024] analyzed long-term observations of CR variations and changes in atmospheric parameters at midlatitudes in Western Siberia (Novosibirsk). The question arises whether the result obtained [Yanchukovsky, 2024] is typical of midlatitudes in general. To answer this question, we have analyzed long-term observations from seven mid-latitude CR stations.

DATA IN USE AND ANALYSIS

Middle latitudes range from the tropic (23°26'22") to the Polar circle (66°33'39") of the corresponding hemisphere. We analyze data from the currently operating CR stations located in this latitude range. The CR stations and their main characteristics are listed in Table 1.

In the column "Geomagnetic cutoff rigidity", the epoch corresponding to a given value is put in brackets. The CR station Oulu is included in the group of mid-latitude stations according to its geographic coordinates, although, in view of the threshold geomagnetic cutoff rigidity (GCR), it should be classified as a high-latitude station. It is grouped with mid-latitude stations in order to trace the latitude effect.

We examine the time interval from 1966 to 2024. On this interval, events with Forbush decreases in galactic cosmic rays with an amplitude ≥2.5 % were selected. In this case, the condition was met that no other FD or solar proton event was observed in the interval ±10 days with respect to the onset of FD. We have thus selected 141 events. Each CR station recorded a different number of events, since observations with neutron monitors at the stations were initiated at different times. There is no pressure data before 1989 in the database for the Irkutsk station, and there is no data on pressure and neutron monitor count rate before 1999 for the Yakutsk station. Initial data shows the count rate of neutron monitors and the simultaneously measured atmospheric pressure. Hourly and daily average values were used. For each monitoring station, Table 2 presents observation intervals, the number of recorded events, the type of instrument, and references to the databases from which the information was taken.

When examining atmospheric temperature variations, we utilize the database [http://crsa.izmiran.ru/phpmyadmin] as a source of hourly upper-air atmospheric sounding data. It contains data from the U.S. National Center for Environmental Prediction NCEP [https://www.nco.ncep.noaa.gov/pmb/products/gfs]. Data on the atmospheric response to FD in CRs was analyzed using the superimposed epoch method, as in [Yanchukovsky, 2024]. The beginning of a decrease in CR intensity in FD was taken as the zero time relative to which

Table 1

Main characteristics of CR stations and references to databases

№	CR station	Coordinates	Altitude, m	Geomagnetic cut-off rigidity, GV	Internet resource
1	Athens, Greece	37.58° N 23.47° E	260	8.348 (2022)	https://www.nmdb.eu/station/athn/ https://tools.izmiran.ru/cutoff/
2	Irkutsk, Russia	52.1° N 104.00° E	475	3.126 (2022)	https://www.nmdb.eu/station/irkt/ https://tools.izmiran.ru/cutoff/
3	Kiel, Germany	54.34° N 10.12° E	54	2.252 (2022)	https://www.nmdb.eu/station/kiel/ https://tools.izmiran.ru/cutoff/
4	Moscow, Russia	55.47° N 37.32° E	200	2.1 (2022)	http://cr0.izmiran.ru/mosc/ https://www.nmdb.eu/station/mosc/ https://tools.izmiran.ru/cutoff/
5	Novosobirsk, Russia	54.84° N 83.00° E	163	2.31 (2022)	https://www.nmdb.eu/station/nvbk/ https://tools.izmiran.ru/cutoff/
6	Oulu, Finland	65.05° N 25.47° E	15	0.718 (2022)	https://www.nmdb.eu/station/oulu/ https://tools.izmiran.ru/cutoff/
7	Yakutsk, Russia	62.02° N 129.72° E	105	1.356 (2022)	https://www.nmdb.eu/station/yktk/ https://tools.izmiran.ru/cutoff/

Table 2

Observation intervals, number of recorded events, type of instrument, and references to databases

№	CR station	Observation period	Number of events	Instrument	Internet resource
1	Athens, Greece	2003–2024	40	6-NM-64	https://www.nmdb.eu/nest/
2	Иркутск, Россия	1989–2024	87	18-NM-64	http://cgm.iszf.irk.ru https://www.nmdb.eu/nest/
3	Kiel, Germany	2011–2024	24	18-NM-64	https://www.nmdb.eu/nest/
4	Moscow, Russia	1966–2024	111	24-NM-64	http://cr0.izmiran.ru/mosc/
5	Novosobirsk, Russia	1968–2024	134	24-NM-64	http://cr0.izmiran.ru/nvbk/main.htm http://193.232.24.200/nvbk/main.htm https://cosm-rays.ipgg.sbras.ru/data-page/
6	Oulu, Finland	1967–2024	128	9-NM-64	https://www.nmdb.eu/nest/ http://cosray.phys.uoa.gr/index.php/esa-neutron-monitor-service/multi-station-neutron-monitor-data
7	Yakutsk, Russia	1999–2024	76	24-NM-64	https://ikfia.ysn.ru/data/hecr/nm/yak

intensity variations of CRs $\Delta I = \frac{I - I_0}{I_0} \cdot 100\,\%$, recorded by a neutron monitor, and changes in atmospheric pressure $\Delta h = h - h_0$. were identified. Here I_0 and h_0 are the neutron monitor count rate and the atmospheric pressure at zero time respectively.

The results thus obtained for each CR station are shown in Figures 1 and 2 for events in cold (see Figures 1, *a* and 2, *a*) and warm (see Figures 1, *b* and 2, *b*) seasons. The interval from October to March was taken for the cold season; and from April to September, for the warm season.

Intensity variations were measured with a standard instrument of the world network of CR stations — a neutron monitor that consists of several identical sections, each with an area of 6 m^2. Monitors at CR stations have a different number of sections (see Table 2) and therefore measure CR intensity variations with unequal accuracy. For example, for the Athens station, where one monitor section operates, the count rate is ~3500 pulse/min, and the error in measuring variations from hourly data runs to 0.22 %. For the Moscow station, where four monitor sections work, the count rate is 8600 pulse/min, and the error in hourly data does not exceed 0.14 %. We use daily averages, so the error in measuring intensity variations for Athens and Moscow decreases to 0.045 and 0.0285 % respectively. The FD effect is about several percent (see Figures 1 and 2). This allows us to use data from all CR stations, including stations with one monitor section. Pressure measurements at the CR stations throughout the time interval were carried out with various instruments: metrological barographs M-22 calibrated twice a day [https://www.анероид.рф/catalog/meteorologiya/registratory/m-22a.htm], digital barographs DB-1.2 developed by ISTP SB RAS [Yanchkovsky et al., 1972], the network working barometer NWB-1M-1 [https://p-barometr.ru/brs-1m]. The error in measurements with the M-22 barograph was ~1 mb. Prototypes of the barograph DB-1 [https://patents.google.com/patent/SU504406A1/ru] were successfully applied for a long time at the stations Irkutsk, Novosibirsk, and Moscow and provided a pressure measurement accuracy of 0.1 mb (10 Pa). Currently, all the stations employ a factory-verified certified barometer NWB-1M (pressure measurement accuracy is 33 Pa). As a result, for the entire observation period the systematic error in pressure measurement did not exceed 1 mb.

The standard error in the average value of ΔI and Δh is defined as $\pm\sigma/\sqrt{n}$ and depends not only on the number of terms n. When a larger number of FDs are recorded, the time interval of observations increases, thereby causing an increase in the range of changes in atmospheric pressure against which the FD effect is observed. This leads to an increase in the standard deviation σ, and therefore there is no sharp decrease in error with a significant increase in the number of detected FDs.

The results obtained at the CR stations are presented in Figures 1 and 2 in descending order of GCR (from low latitudes to high latitudes). When the CR intensity

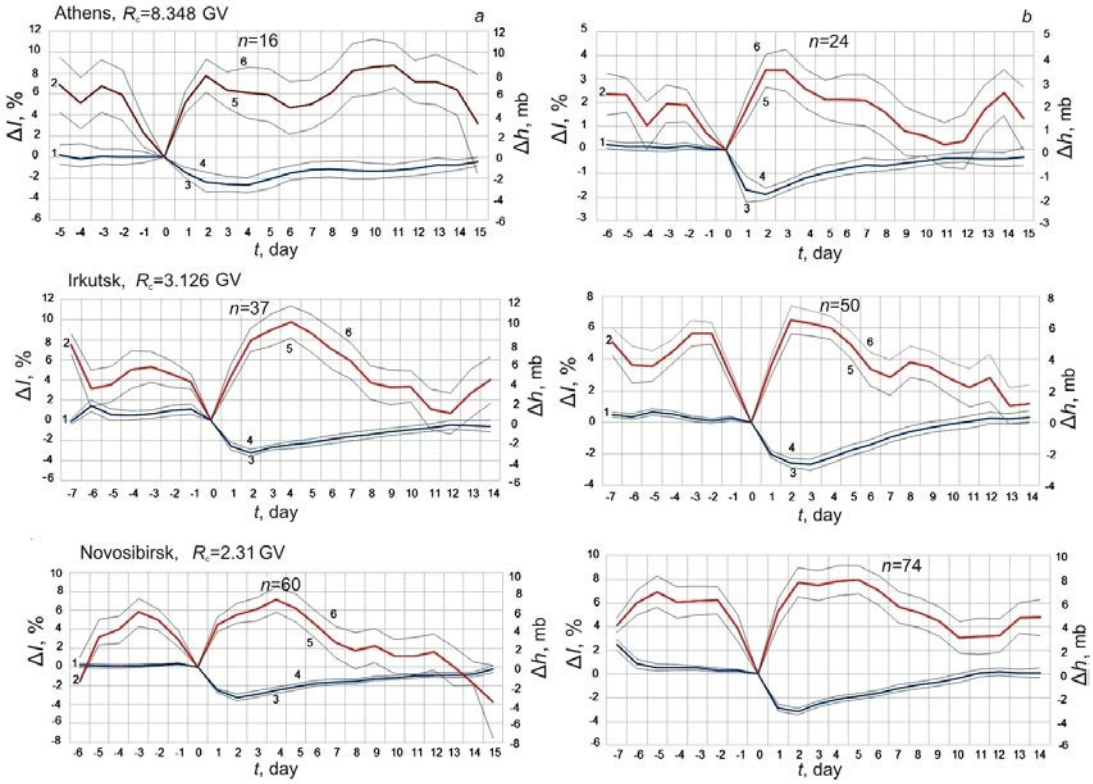

Figure 1. Variations in CR intensity ΔI (curve 1) and atmospheric pressure Δh (curve 2) for cold (*a*) and warm (*b*) seasons observed at CR stations with threshold rigidities from 8.348 to 2.31 GV. Curves 3, 4, and 5, 6 show standard errors of the mean for ΔI and Δh respectively

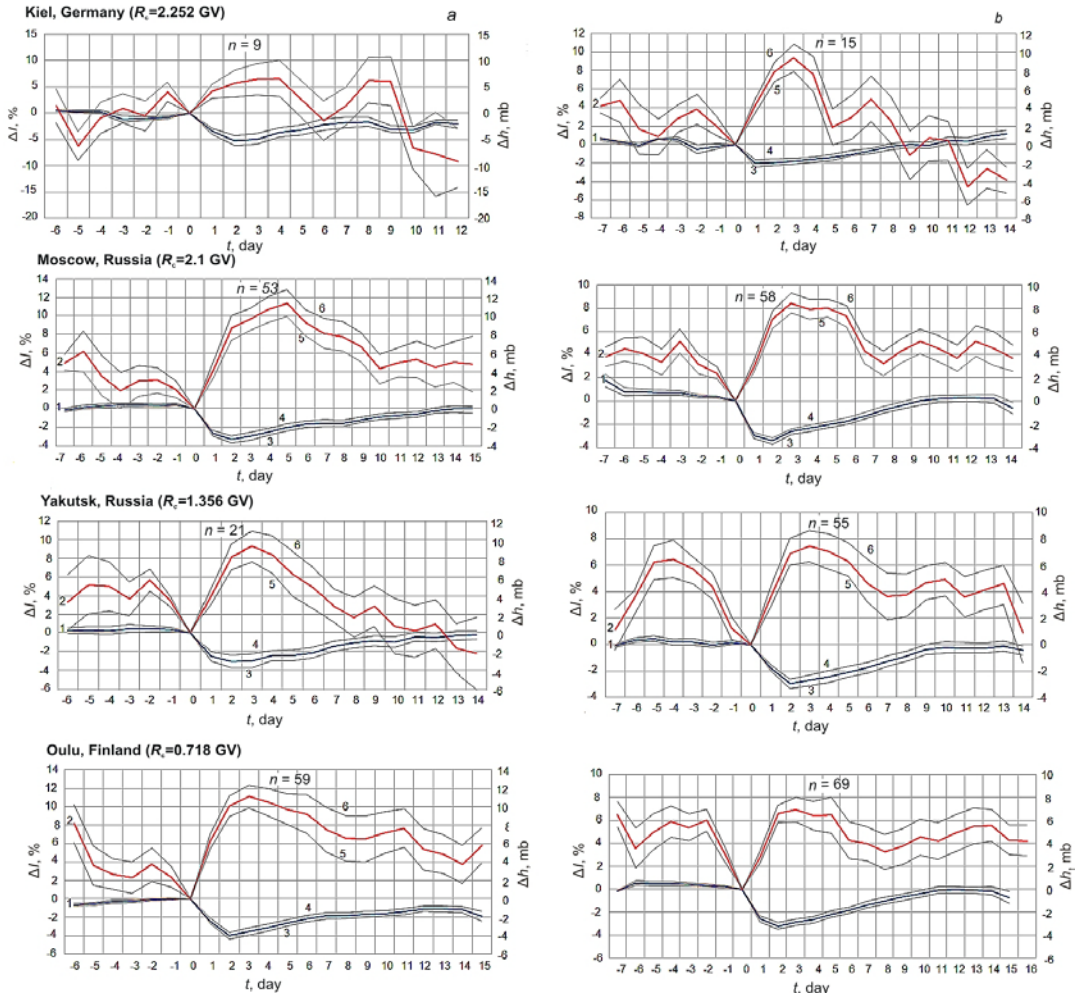

Figure 2. Variations in CR intensity Δ*I* (curve 1) and atmospheric pressure Δ*h* (curve 2) for cold (*a*) and warm (*b*) seasons observed at CR stations with threshold rigidities from 2.252 to 0.718 GV. Curves 3, 4, and 5, 6 show standard errors of the mean for Δ*I* and Δ*h* respectively

decreases and is minimum during FD, the atmospheric pressure rises (relative to zero day) at all mid-latitude stations at any time of the year. When the CR intensity recovers after FD, the pressure falls. The duration of this atmospheric response coincides with the duration of FD in CRs. Note that the effect is more pronounced during the cold period, as well as for CR stations with small GCR values. Atmospheric pressure increases to maximum values on the 3d–5th days. For CR stations with small GCR values, the pressure often has a maximum on the third day already. The CR intensity and atmospheric pressure variations during FD, averaged over all mid-latitude CR stations and all events, are plotted in Figure 3.

The averaging over all CR stations was performed with regard to their statistical weight, i.e. taking into account the proportion of events recorded at each station in the total number of events. In practice, the results are considered reliable if the level of statistical significance of the results is <0.05, which corresponds to a confidence interval ±3σ. The standard deviations $\sigma = \sqrt{\frac{1}{n}\sum_{i=1}^{n}\left(\Delta h_i - \overline{\Delta h}\right)^2}$ were found, as in [Yanchukovsky, 2024], independently for each point of the obtained distributions. There is a spread of σ values: for the events in the cold season, in the range 0.144–0.5 with an average value of 0.378; for the events in the warm season, in the range 0.135–0.3 with an average value of 0.233; for all events, in the range 0.139–0.35 with an average value of 0.279. Before FD, the atmospheric pressure decreases. This pressure behavior, i.e. its decrease before the FD front, was also observed earlier [Tinsley et al., 1989]. It was suggested that this should be considered as a separate effect of a solar flare that triggers FD in CRs (the so-called early and late flare effects) [Tinsley et al., 1989].

The atmospheric pressure during FD generally rises on the first three days when the CR intensity decreases sharply. Pressure variations Δ*h* reach a maximum on the fourth or fifth day, then Δ*h* goes down during the CR intensity recovery phase after FD. The pressure drop averages 8 mb. Thus, the effect is more pronounced in the cold season. Earlier in [Mustel, 1974; Tinsley, Deen, 1991; Veretenenko, Thejll, 2013], it was indicated that the atmospheric response to changes in solar activity at moderate latitudes of the Northern Hemisphere is more pronounced during the cold season when cyclonic processes intensify due to increased temperature contrasts in the troposphere.

The superimposed epoch method was employed to

study the atmospheric temperature behavior at mid-latitudes during FD in CRs. The vertical profile of atmospheric temperature was obtained from aerological data with hourly resolution from databases [http://crsa.izmiran.ru/phpmyadmin, https://www.nco.ncep.noaa.gov/pmb/products/gfs], where, unfortunately, data is available only for the period from 2000 to 2018 for four CR stations: Kiel, Moscow, Novosibirsk, and Yakutsk. The mean mass atmospheric temperature $T_{\text{mm}} = \sum_{i=1}^{n} T_i \Delta h_i \Big/ \sum_{i=1}^{n} \Delta h_i$ was utilized as a characteristic of the temperature regime of the atmosphere, where T_i is the temperature of the atmospheric layer (isobars) i, and Δh_i is the mass of this layer, as well as the surface temperature T_{surf} (temperature of the surface layer of variable mass (h–950) mb). The total number of FDs recorded by the four CR stations during the given period was 112, 20 of which were detected by the Kiel station; 29, by the Moscow station; 35, by the Novosibirsk station; and 30, by the Yakutsk station. Variations in the mean mass ΔT_{mm} and surface ΔT_{surf} temperatures during FDs for these observation stations are illustrated in Figure 4.

The mean mass and surface temperature variations observed at all CR stations have significant differences in the cold and warm seasons. Atmospheric temperature variations are more pronounced during the cold season. When the CR intensity decreases during FD, mean mass and surface temperatures go up, whereas during the CR intensity recovery phase in FD, on the contrary, the atmospheric temperature goes down. The CR intensity and mean mass and surface atmospheric temperature variations during FDs in CRs, averaged over four mid-latitude CR stations and all events, are plotted in Figure 5.

As before, the averaging over all CR stations was performed taking into account their statistical weight. Deviations σ for ΔT_{mm} (for the cold period) are in the range 0.078–0.31 with an average value of 0.214; and for ΔT_{surf}, in the range 0.108–0.42 with an average value of 0.306.

When the CR intensity decreases during FD, the atmospheric pressure, mean mass and surface temperatures rise, reaching the highest values at minimum CR intensity (near minimum FD), and then these parameters decrease with increasing CR intensity (during the FD recovery phase). In the cold season, the mean mass temperature of the atmosphere rises by an average of one degree: ΔT_{mm}=+1.11 °C. The rise in the surface temperature is almost twice as high: ΔT_{surf}=+1.86 °C.

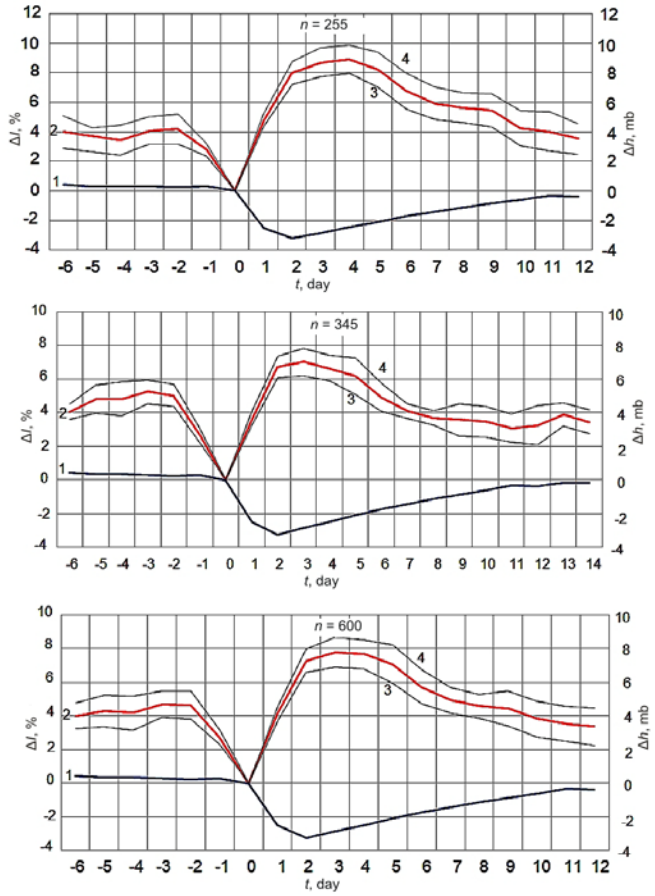

Figure 3. Variations in CR intensity ΔI (curve 1) and atmospheric pressure Δh (curve 2) during FD at midlatitudes for events during cold (*a*) and warm (*b*) seasons and for all events (*c*). Curves 3 and 4 denote boundaries of the ±3σ confidence interval

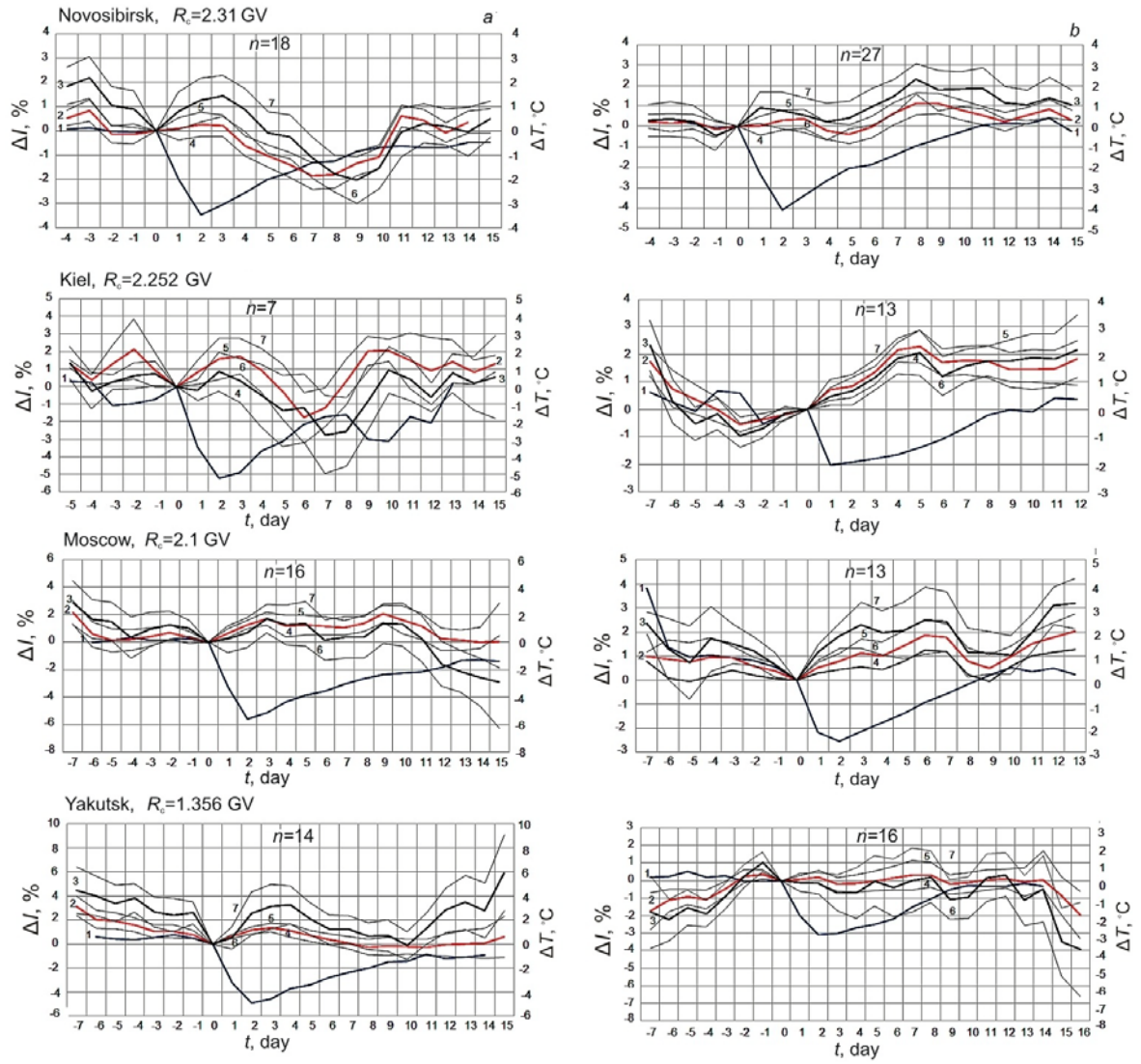

Figure 4. Variations in CR intensity ΔI (curve 1) and mean mass (curve 2) and surface (curve 3) temperatures of the atmosphere ΔT during FD in CRs observed at four mid-latitude CR stations during cold (*a*) and warm (*b*) seasons. Curves 4, 5, and 6, 7 show standard errors of the mean for ΔT_{mm} and ΔT_{surf} respectively

Forbush decreases in cosmic rays feature significant CR intensity variations (drastic decline and gradual recovery) that cause abrupt changes in the atmospheric ionization rate and hence changes in the chemical and aerosol composition of the atmosphere, which leads to changes in atmospheric transparency and cloudiness [Pudovkin, Raspopov, 1993]. It is noted [Shumilov et al., 1996] that this happens without a significant time delay.

The results suggest that changes in the cloudiness and transparency of the atmosphere triggered by changes in the ionization rate during FDs in CRs produce the observed effects. A decrease in cloudiness during FDs in CRs at moderate and high latitudes has been found in [Veretenenko, Pudovkin, 1994, 1996; Todd, Kniveton, 2001, 2004]. Changes in atmospheric cloudiness and transparency regulate the amount of both incoming short-wave solar radiation to the Earth surface and long-wave radiation emitted by the Earth surface. The total effect in this case is determined by latitude, time of year, and type of the Earth surface (mainland, ocean) [Matveev, 1991].

The effect of solar activity on the tropospheric temperature was examined in [Karakhanyan, Molodykh, 2018], using geomagnetic activity indices as an indicator of solar activity. FDs in CRs often occur during geomagnetic disturbances, but not always. Some FDs are not accompanied by geomagnetic storms, and some geomagnetic disturbances occur without FDs. Going forward, this can allow us to classify all events according to this feature, by dividing them into three categories and studying them independently.

CONCLUSION

During Forbush decreases in cosmic rays (at decreased and minimum CR intensity), a rise in atmospheric pressure is observed at all mid-latitude CR stations. When the CR intensity recovers after FD, the pressure falls. The duration of this atmospheric response coincides with the duration of FD in CRs. Note that the effect is more pronounced during the cold period, as well as for CR stations with small GCR values. A rise in atmospheric pressure is generally recorded on the first

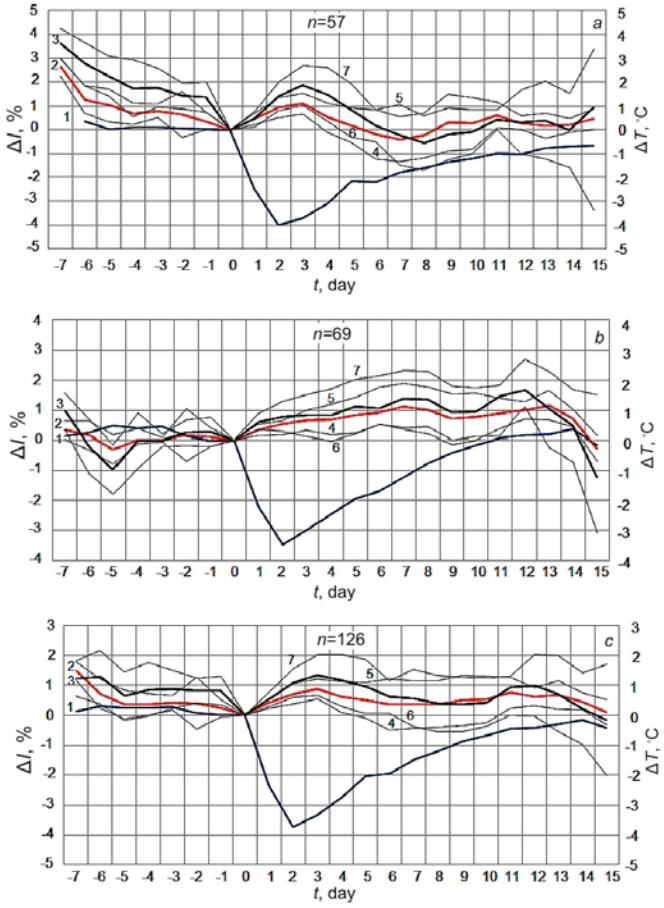

Figure 5. Variations in CR intensity Δ*I* (curve 1) and mean mass (curve 2) and surface (curve 3) temperatures of the atmosphere Δ*T* during FDs in CRs for events in cold (*a*) and warm (*b*) seasons and for all events (*c*). Curves 4, 5, and 6, 7 indicate boundaries of the ±3σ confidence interval for ΔT_{mm} and ΔT_{surf} respectively

three days when the CR intensity drops sharply. Pressure variations Δ*h* peak on the fourth or fifth day. For CR stations with small GCR values, the pressure often has a maximum on the third day already. The pressure drop Δ*h* for moderate latitudes averages 8 mb.

Variations in the mean mass and surface temperatures during FDs in CRs are observed at all CR stations and differ significantly for cold and warm seasons. When the CR intensity decreases during FD, atmospheric pressure, mean mass and surface temperatures rise, reaching the highest values at minimum CR intensity (near minimum FD), and then these parameters decrease with increasing CR intensity (during the FD recovery phase).

The work was financially supported by the Ministry of Science and Higher Education of the Russian Federation (Project FWZZ-2022-0019). The results were obtained using the equipment of Unique Research Facility 85 “Russian National Network of Cosmic Ray Stations” [http://www.ckp-rf.ru/usu/433536].

REFERENCES

Dickinson R.E. Solar variability and the lower atmosphere. *Bulletin of the American Meteorological Society*. 1975, vol. 56, iss. 12, pp. 1240–1248. https://doi.org/10.1175/1520-0477(1975)056<1240:SVATLA>2.0.CO;2.

Erlykin A.D., Wolfendale A.W. Cosmic ray effects on cloud cover and their relevance to climate change. *J. Atmos. Solar-Terr. Phys.* 2011, vol. 77, pp. 1681–1686. https://doi.org/10.1016/j.jastp.2011.03.001.

Erlykin A.D., Gualai G., Kudela K., Sloan T., Wolfendale A.W. Some aspects of ionization and the cloud cover, cosmic ray correlation problem. *J. Atmos. Solar-Terr. Phys.* 2009, vol. 71, pp. 823–829. https://doi.org/10.1016/j.jastp.2009.03.007.

Karakhanyan A.A., Molodykh S.I. Spatial distribution of temperature during geomagnetic disturbances. *Sol.-Terr. Phys.* 2018, vol. 4, iss. 4, pp. pp. 59–62. https://doi.org/10.12737/stp-44201808.

Kniveton D.R. Precipitation, cloud cover and Forbush decreases in galactic cosmic rays. *J. Atmos. Solar-Terr. Phys.* 2004, vol. 66, iss. 13-14, pp. 1135–1142. https://doi.org/10.1016/j.jastp.2004.05.010.

Kondratyev K.Ya., Nikolsky G.A. The solar constant and climate. *Solar Phys.* 1983, vol. 89, pp. 215–222. https://doi.org/10.1007/BF00211964.

Kudryavtsev I.V., Jungner H. Variations in atmospheric transparency under the action of galactic cosmic rays as a possible cause of their effect on the formation of cloudiness. *Geomagnetism and Aeronomy*. 2011, vol. 51, iss. 5, pp. 656–663. https://doi.org/10.1134/S0016793211050100.

Matveev L.T. *Theory of General Circulation of the Atmosphere and Climate of the Earth*. Leningrad, Gidrometeoizdat Publ., 1991, 296 p. (In Russian).

Mustel E.R. Current state of the question about the reality of cor-

puscular-atmospheric connections. *Solar-Atmospheric Connections in Climate Theory and Weather Forecasts*. Leningrad, Gidrometeoizdat Publ., 1974, pp. 7–18. (In Russian).

Pudovkin M.I., Raspopov O.M. The mechanism of the impact of solar activity on the state of the lower atmosphere and meteorological parameters (review). *Geomagnetism and Aeronomy*. 1992, vol. 32, pp. 1–22. (In Russian).

Pudovkin M.I., Raspopov O.M. Physical mechanism of the action of solar activity and other geophysical factors on the state of the lower atmosphere, meteorological parameters, and climate. *Physics - Uspekhi*. 1993, vol. 163, iss. 7, pp. 664–647. https://doi.org/10.1070/PU1993v036n07ABEH002296.

Pudovkin M.I., Veretenenko S.V. Cloudiness decreases associated with Forbush-decreases of galactic cosmic rays. *J. Atmos. Solar-Terr. Phys.* 1995, vol. 57, iss. 11, pp. 1349–1355. https://doi.org/10.1016/0021-9169(94)00109-2.

Pudovkin M.I., Veretenenko S.V., Pellinen R., Kyro E. Meteorological characteristic changes in the high-latitudinal atmosphere associated with Forbush decreases of galactic cosmic rays. *Adv. Space Res.* 1997, vol. 20, iss. 6, pp. 1169–1172. https://doi.org/10.1016/S0273-1177(97)00767-9.

Pudovkin M.I., Veretenenko S.V., Pellinen R., Kyro E. Cosmic ray variation effects in the temperature of the high-latitude atmosphere. *Adv. Space Res.* 1996, vol. 17, iss. 11, pp. 165–168. https://doi.org/10.1016/0273-1177(95)00746-2.

Roldugin V.C., Tinsley B.A. Atmospheric transparency changes associated with solar wind-induced atmospheric electricity variations. *J. Atmos. Solar-Terr. Phys.* 2004, vol. 66, iss. 13-14, pp. 1143–1149. https://doi.org/10.1016/j.jastp.2004.05.006.

Shumilov O.I., Kasatkina E.A., Henriksen K., Vashenuk E. Enhancement of stratospheric aerosol after solar proton event. *Ann. Geophys*. 1996, vol. 4, iss. 11, pp. 1119–1123. https://doi.org/10.1007/s00585-996-1119-y.

Tinsley B.A., Deen G.W. Apparent tropospheric response to MeV-GeV particle flux variations: a connection via electrofreezing of supercooled water in high-level clouds? *J. Geophys. Res.* 1991, vol.96, pp. 22283−22296. https://doi.org/10.1029/91JD02473.

Tinsley B.A., Brown G.M., Scherrer P.H. Solar variability influences on weather and climate: Possible connections through cosmic ray fluxes and storm intensification. *J. Geophys. Res.* 1989, vol. 94, iss. D12, pp. 14783–14792. https://doi.org/10.1029/JD094iD12p14783.

Todd M.C., Kniveton D.R. Changes in cloud cover associated with Forbush decreases of galactic cosmic rays. *J. Geophys. Res.* 2001, vol. 106, pp. 32031–32041. https://doi.org/10.1029/2001JD000405.

Todd M.C., Kniveton D.R. Short term variability in satellite-derived cloud cover and galactic cosmic rays: an update. *J. Atmos. Solar-Terr. Phys.* 2004, vol. 66, pp. 1205–1212. https://doi.org/10.1016/j.jastp.2004.05.002.

Veretenenko S.V., Pudovkin M.I. Effects of Forbush declines of galactic cosmic rays on total cloud cover variations. *Geomagnetism and Aeronomy*, 1994, vol. 34, pp. 38–44 (In Russian).

Veretenenko S.V., Pudovkin M.I. Variations in total cloudiness during solar cosmic ray bursts. *Geomagnetism and Aeronomy*. 1996, vol. 36, iss. 1, pp. 153–156. (In Russian).

Veretenenko S.V., Tejll P. Solar proton events and evolution of cyclones in the North Atlantic. *Geomagnetism and Aeronomy*. 2008, vol. 48, iss. 4, pp 518–528. https://doi.org/10.1134/S0016793208040130.

Veretenenko S.V., Ogurtsov M.G. Study of spatial and temporal structure of long-term effects of solar activity and cosmic ray variations on the lower atmosphere circulation. *Geomagnetism and Aeronomy*. 2012, vol. 52, iss. 5, pp. 591–602. https://doi.org/10.1134/S0016793212050143.

Veretenenko S., Thejll P. Influence of energetic Solar Proton Events on the development of cyclonic processes at extratropical latitudes. *IOP Publishing. J. Phys.: Conf. Ser.* 2013, vol. 409, 012237. https://doi.org/10.1088/1742-6596/409/1/012237.

Yanchukovsky A.L., Tergoev V.I., Shapovalova P.A. Digital barograph. Patent SU504406A1. 1972.

Yanchukovsky V.L. Response of the mid-latitude atmosphere to sporadic cosmic ray variations in the Western Siberian region. *Sol.-Terr. Phys.* 2024, vol. 10, iss. 4, pp. 59–64. https://doi.org/10.12737/stp-104202407.

URL: http://crsa.izmiran.ru/phpmyadmin (accessed September 17, 2025).

URL: https://www.nco.ncep.noaa.gov/pmb/products/gfs (accessed September 17, 2025).

URL: https://www.nmdb.eu/station/athn/ (accessed September 18, 2025).

URL: https://www.nmdb.eu/station/irkt/ (accessed September 18, 2025).

URL: https://www.nmdb.eu/station/kiel/ (accessed September 18, 2025).

URL: http://cr0.izmiran.ru/mosc/ (accessed September 18, 2025).

URL: https://www.nmdb.eu/station/mosc/ (accessed September 18, 2025).

URL: https://www.nmdb.eu/station/nvbk// (accessed September 18, 2025).

URL: https://www.nmdb.eu/station/oulu/ (accessed September 18, 2025).

URL: https://www.nmdb.eu/station/yktk/ (accessed September 18, 2025).

URL: https://www.nmdb.eu/nest/ (accessed September 18, 2025).

URL: http://cgm.iszf.irk.ru (accessed September 18, 2025).

URL: http://cr0.izmiran.ru/nvbk/main.htm (accessed September 18, 2025).

URL: http://193.232.24.200/nvbk/main.htm (accessed September 18, 2025). https://www.nmdb.eu/station/mosc/

URL: https://cosm-rays.ipgg.sbras.ru/data-page/ (accessed September 18, 2025).

URL: http://cosray.phys.uoa.gr/index.php/esa-neutron-monitor-service/multi-station-neutron-monitor-data (accessed September 18, 2025).

URL: https://ikfia.ysn.ru/data/hecr/nm/yak (accessed September 18, 2025).

URL: http://www.ckp-rf.ru/usu/433536 (accessed October 25, 2025).

URL: https://tools.izmiran.ru/cutoff/ (accessed October 25, 2025).

URL: https://p-barometr.ru/brs-1m (accessed October 25, 2025).

URL: https://patents.google.com/patent/SU504406A1/ru (accessed October 25, 2025).

URL: https://www.анероид .рф/catalog/meteorologiya/registratory/m-22a.htm (accessed October 25, 2025).

Original Russian version: Yanchukovsky V.L., Kuzmenko V.S., Khisamov R.Z., published in Solnechno-zemnaya fizika. 2026, vol. 12, no. 2, pp. 54–62. https://doi.org/10.12737/szf-122202606.

How to cite this article

Yanchukovsky V.L., Kuzmenko V.S., Khisamov R.Z. The mid-latitude atmosphere during Forbush decreases in cosmic rays. *Sol.-Terr. Phys.* 2026, vol. 12, iss. 2, pp. 49–56. https://doi.org/10.12737/stp-122202606.